

25th ABCM International Congress of Mechanical Engineering
October 20-25, 2019, Uberlândia, MG, Brazil

COB-2019-1232

BIO-INSPIRED AND EVOLUTION ALGORITHMS - PID CONTROLLER TUNING, APPLIED TO A MOTOR-ELECTRIC DYNAMETER SYSTEM

Leonardo Bezerra Libanio

Postgraduate program in Mechatronic Systems University of Brasilia. Darcy Ribeiro, CEP: 70910-900 Brasilia, DF, Brazil
e-mail: bezerralibanio@gmail.com

Rudi van Els

University of Brasilia, Campus Universitário Darcy Ribeiro, Brasília, Brazil
e-mail: rudi@unb.br

Summary: *The aim of this paper is to analyze and test bio-inspired optimization algorithms in swarm intelligence and differential evolution to solve PID tuning problems in motor-dynamometer cost function resolution. The methodology used is defined in 03 steps. In the first step the algorithms are described; Particle Swarm Optimization - PSO and Differential Evolution Optimization - DE; and the cost function that represents the optimization problem. In the second step the results and discussions of the simulations performed with the development tool Matlab and Simulink will be presented. In the third step the results and discussions of the tests performed with the cost optimized function to control the internal combustion motor-electric dynamometer system will be presented. The selected cost function is nonlinear with representation from a transfer function of a motor-dynamometer system. In order to better observe the performance of the algorithms in the tests, the results obtained in the frequency and power control with characteristic tests for path tracking will be presented graphically.*

Key words: *Bio-inspired algorithms, swarm intelligence, PID, Cost Function.*

1. INTRODUCTION

The definition of mathematical optimization is the capability to accomplish the best possible result within a set of solutions in a finite or infinite space in order to minimize efforts or maximize profits. With the purpose of verifying if a solution is optimal, it is required to acquire a mathematical representation, called “objective function” or “cost function”, which allows evaluating each solution. This representation is formed by one or several decision variables and a set of constraints that affect the optimization problem. Accordingly, the goal of optimization is to find the best or acceptable value of the cost function (the largest possible numerical value implies maximization and the smallest possible numerical value implies minimization) (Serapião, 2009).

Problems comprising global optimization over continuous spaces permeate the scientific community. On the whole, the task is to optimize certain properties of a system by choosing the system parameters as a result. For convenience, the system parameters are customarily represented as a vector. The standard approach to an optimization problem begins by designing a cost function that can model the problem objectives while incorporating constraints. (Storn and Price, 1995).

Bio-inspired algorithms are optimization techniques broadly used in recent years to solve complex multi-variable problems in which robust solutions are difficult or impossible to find using classical (gradient calculus based) methods. This type of algorithm mimics the social behavior of some species of nature, nonetheless precisely of species that have collective intelligence. The key feature of these algorithms is the process of interaction between swarm individuals who are based on simple rules, but use their collective intelligence capabilities to perform complex tasks. (Diago, 2015).

Following, the article describes: The bio-inspired algorithms PSO and evolution DE, the electric motor-dynamometer cost function, the results and discussions of the algorithm tests based on graphs and statistical data, the results and discussions of the path tracking tests with the components P, I and D and finally the conclusion.

2. BIO-INSPIRED ALGORITHMS IN SWARM INTELLIGENCE AND DIFFERENTIAL EVOLUTION

2.1 Particle Swarm Optimization - PSO

Basic PSO algorithm can generally be described as a set of vectors enclosing data linked to the position of the particles, which move in a region or defined area (see Fig. 01). In this algorithm, the new position of a particle is

defined by its particular experience, known as individual memory (the particle remembers the best position determined by evaluating the cost function). Similarly, the particle is influenced by the overall swarm experience, known as collective memory (the particle remembers the best swarm position determined by the best aptness when assessed in the cost function.) (Eberhart and Kennedy, 1995).

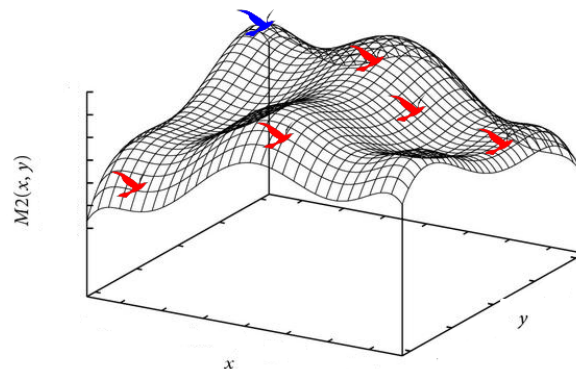


Figure 1 – Moving vectors set

Source: Adapted from <http://computacaointeligente.com.br/algoritmos/otimizacao-por-enxame-de-particulas> (2019).

2.2 Optimization by Differential Evolution – DE

This algorithm uses NP D-dimensional parameter vectors $x_i, G, i = 1, \dots, NP$, as population in each generation G .

The initial set of vectors is randomly generated and should cover the entire search space. In the absence of any knowledge about the search space (promising regions or even partial solutions), a uniform distribution for the initial population is used. (Rahnamayan et. al., 2006).

DE generates new parameter vectors by adding the weighted difference between two parameter vectors to a third individual. Consider this operation as a mutation.

The mutated parameter vectors are then combined with other predetermined vectors, called target vectors, to generate the trial vectors. This parameter combination is referred to as crossover in DE. It is important to underscore that each vector present in the current population should be used once as a trial vector.

If the trial vector provides a higher fitness value (maximization) than that associated with the respective target vector, the latter will give way to the first in the next generation. This operation corresponds to the selection.

Mutation process: For each target vector $x_i, G, i = 1, \dots, NP$, a new vector is generated by Eq. 1.

$$v_{i,G+1} = x_{r1,G} + F(x_{r3,G} - x_{r2,G}) \tag{1}$$

Where $r1, r2, r3 \in 1, 2, \dots, NP$ are mutually distinct indexes and also different from the index i .

F is a real constant $\in [0, 2]$ that determines the size of the step to be taken in the direction defined by the difference vector: $x_{r3,G} - x_{r2,G}$. Be x_i, G the current *target vector* (see Fig. 02).

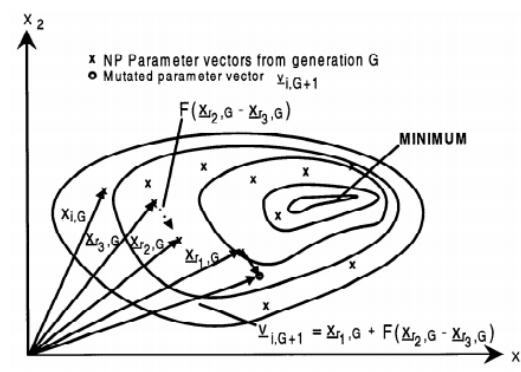


Figure 2 - Two-dimensional mutation process.

Source: Storn and Price, (1995).

2.3 Algorithm Performance Upgrading Techniques

These methods are modifications made by researchers pursuing to increase the performance of population-based algorithms. Methods known in the literature as the addition of artificial diversity try to avoid the problem of premature convergence, particularly when using topologies in which swarm agents exclusively follow the best performing individual. For such cases there is a strong tendency to find suboptimal solutions as a consequence of the best individual being confined in a minimum space (Karaboga and Basturk, 2007).

It is important to know that, with these modifications, the performance of the algorithms can be improved, but the computational complexity of the algorithm is also augmented. The methods presented in this paper among the many that can be found in the literature are: 1) Inertia factor; 2) Constriction factors; 3) Opposition Learning Variations (OBL); and 4) Attractive-Repulsive (RA).

1) Inertia factor: is applied during speed calculation and is used as a scale factor for the current speed of each particle, see equations 2 and 3 (Shi and Eberhart, 1999).

$$v_{ij}^{(t+1)} = wv_{ij}^{(t)} + \underbrace{c_1 U_{1j}[0,1]}_{\text{cognitive component}} (y_{ij}^{(t)} - x_{ij}^{(t)}) + \underbrace{c_2 U_{2j}[0,1]}_{\text{social component}} (y_{sj}^{(t)} - x_{ij}^{(t)}) \quad (2)$$

$$x_{ij}^{(t+1)} = x_{ij}^{(t)} + v_{ij}^{(t+1)} \quad (3)$$

This technique is broadly used, setting the inertia factor w to linearly decrease from large values to small values throughout the execution of the algorithm. Typical values: $w=[0.9 \text{ to } 0.1]$.

- Inertia factor controls the particle exploration capability.
- Large values of w result in a global search.
- Small values of w allow particles to locally explore the neighborhood of a possible solution.
- The PSO algorithm using the inertia factor w and coefficients c_1 and c_2 is academically known as canonical PSO algorithm.

2) Constriction factors: useful for ensuring convergence in the algorithm. Constriction factor makes it easy to choose parameters w , c_1 and c_2 through the following relations (see equations 4 and 5).

$$v_{ij}^{(t+1)} = x(v_{ij}^{(t)} + c_1 U_{1j}(y_{ij}^{(t)} - x_{ij}^{(t)}) + c_2 U_{2j}(y_{sj}^{(t)} - x_{ij}^{(t)})) \quad (4)$$

$$x = 2 / |2 - \phi - \sqrt{\phi^2 - 4\phi}| \quad (5)$$

where, $\phi = c_1$ and c_2 , $\phi > 4$

As a result, PSO can be applied without imposing restrictions on the particle path, specifically the V_{max} value.

- The most widely found common constriction method in the literature is to use $f=4.1$ with constants $c_1=c_2=2.05$ ($c=0.729$) (DIAGO, 2015).

3) Opposition Learning Variation (OBL)

The opposition learning method, which directs the search for the best solution by the bio-inspired algorithms, in the opposite direction of the current search. This process consists that at a given moment the agents are together around the best position found, with a decrease in diversity. In this case, this technique allows to change the positions of some of its agents to opposite coordinates, exploring new possibilities in the search space. (Rahnamayan et. al., 2008).

The OBL approach is based on the concept of the opposite number, defined by eq. 06.

$$\hat{x} = a + b - x \quad (6)$$

where x is a real number defined in the range $[a,b]$ and \hat{x} the opposite number of x . This definition is also valid for N -dimensional points x_i defined in the range. $[a_i, b_i]$, $i = 1, 2, \dots, N$ [07].

2.4 Cost Function - Problem Description

Internal combustion engines (MCI) stand out in the automotive, industrial and power generation sectors, the study seeks to corroborate the potential use of control optimization techniques to increase performance using the electric dynamometer for tests typical of the path tracking. Fig. 03 shows the internal combustion motor-electric dynamometer control system.

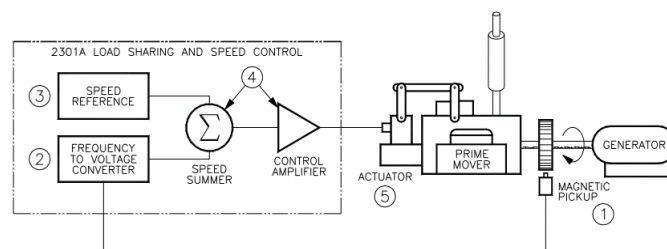


Figure 03 – MCI Control System – Electric Dynamometer.

Available from: <https://www.woodward.com/en/search?q=82389&o=Title,Ascending&e=0>.

The turbocharged direct-injection four-stroke internal combustion diesel motor with intermediate cooling system (water) with the following main features: V-configuration, 12 cylinders, 460 mm cylinder bore, speed 1200 rpm, average piston speed 9.9 m/s, 167 kW power per cylinder at 1200 rpm, 02 inlet valves, 02 outlet valves, right-hand steering direction and manufacturer Wartsila.

The three-phase electric dynamometer has the following main features: 2,500 kVA apparent power, 2000 kW active power, 4,160 VAC voltage, 60 Hz frequency, 347 A electric current, 1800rpm rotation and manufacturer Leroy Somer.

The 2301A Speed Controller manufactured by Woodward controls the speed and load of the diesel engine in isochronal mode, as shown in Fig. 03, the control system consists of:

- 1 - Magnetic sensor to detect main motor speed;
- 2 - Frequency to voltage converter;
- 3 - Main engine speed reference (1200 rpm);

4 - Speed amplifier with output proportional to the amount of fuel required to maintain the reference speed and load of the required by the power system. The speed signal voltage is compared to the reference voltage at the sum point. If the speed signal voltage is less than or greater than the reference voltage, a signal is sent from the control amplifier, demanding an increase or decrease in speed;

5 - Actuator to position the fuel engine (injector rack) of the primary engine, thus maintaining the reference speed and load required by the power system;

In isochronal mode - Speed regulators are used in power systems to regulate the speed of an engine, and so the frequency of the synchronous generator voltage at which a disturbance has occurred. This disturbance happens continuously because the power demand is variable. It is a mode in which it is possible to control the power and frequency of a system and for the speed to be kept at the desired value it is required that the power generated is equal to the load power.

2.4.1 PID Function

PID (Proportional Integral Derivative) control is one of the most universally used techniques when controlling continuous variables. PID control consists of a mathematical algorithm, which has as its function the precise control of a variable in a system, allowing the system to operate stably at the desired setpoint, even if variations or disturbances that would affect its stability occur, as shown. Fig. 04.

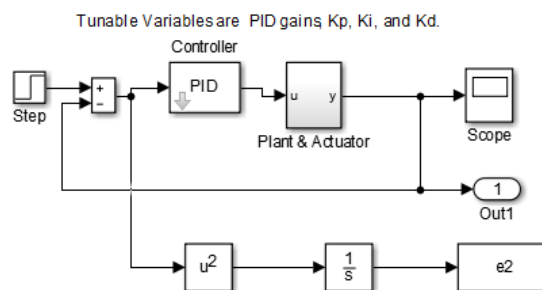


Figure 4 – PID controller block diagram

Source: By author, 2019.

PID control can be described by Eq. 7, where K_p is the proportional gain, E is the error, K_i is the integral gain, K_d is the derivative gain and MV is the manipulated variable.

$$MV = K_p \times E + K_i \int_0^t E \times dt + K_p K_d \frac{dE}{dt} S_0 \quad (7)$$

2.4.2 Plant Modeling

The motor-dynamometer system assessed can be described according to Fig. 5, and its transfer function is attained from deductions, Laplace transform applications and considering initial conditions.

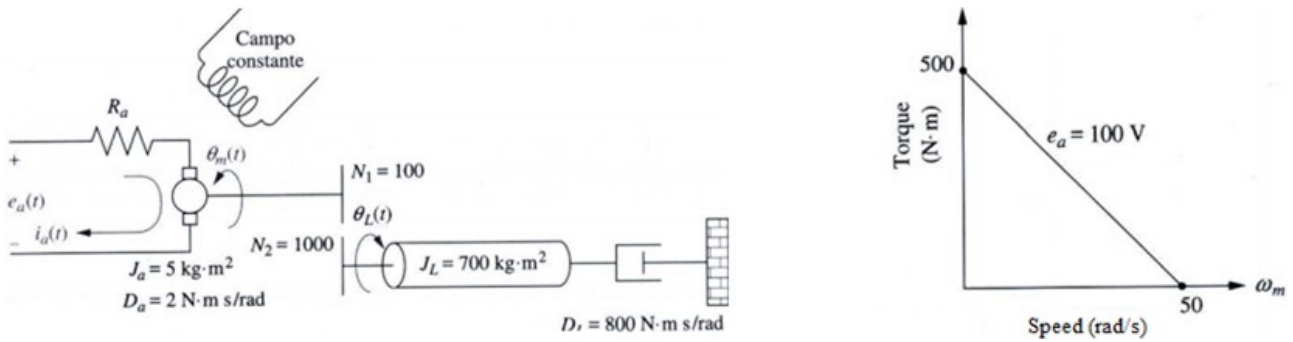


Figure 5 – Engine-dynamometer system
Source: Quevedo (2012).

And it results in the motor-dynamometer transfer function, used in the PID controller tuned via PSO, DE bio-inspired algorithms and OBL learning variations, simulated via the Matlab and Simulink tool. The transfer function is represented according to Eq. 8, being the output offset representation generated (θ_L) by an electrical input (E_a).

$$\frac{\theta_L}{E_a} = \frac{0.0417}{s(s + 1.667)} \quad (8)$$

3. RESULTS AND DISCUSSIONS OF SIMULATIONS OF BIO-INSPIRED AND EVOLUTION OPTIMIZATION ALGORITHMS ACCORDING TO COST FUNCTION

The results of the optimization algorithm tests are presented statistically in tables containing the mean, median, standard deviation of the obtained data, minimum value and number of hits, as well as the values found for the PID components. For each PSO and DE algorithm and OBL learning variations the configuration parameter values are shown in Table 1.

Table 1. Configuration parameters of the algorithms DE, PSO, O-PSO and O-DE

DE		PSO		O-PSO		O-DE	
PARAMETERS	VALUE	PARAMETERS	VALUE	PARAMETERS	VALUE	PARAMETERS	VALUE
Swarm size	[20]	Swarm size	[20]	Swarm size	[20]	Swarm size	[20]
Dimensions	3	Dimensions	3	Dimensions	3	Dimensions	3
Interactions	100	Interactions	100	Interactions	100	Interactions	100
Mutation factor	1,2	Inertia weight	0,9 a 0,1	Inertia weight	0,9 a 0,1	Mutation factor	1,2
Crossover rate	1	Social & cognitive coefficient	C1=C2= 2,05	Social & cognitive coefficient	C1=C2= 2,05	Crossover rate	1
		Maximum speed	-3,3	Maximum speed	-3,3		
				Limit	40	Limits	40

Source: By author, 2019.

The algorithms were executed 32 times for each parameter set (number of particles and number of dimensions). For the 32 executions the initial positions of the agents were randomly generated. From the results obtained in each test was chosen the best position found by the particles and their suitability value (minimum value found). The results of the 32 experiments calculated the mean, median, minimum value, standard deviation and nonparametric performance tests for each algorithm. The results are described in Table 02.

Table 2. Statistical results of the algorithms

ALGORITHM		AVERAGE	MEDIAN	MINIMUM	STANDARD DEVIATION	GOALS / 32	P	I	D
S=20 N=3	PSO	-1,00E+38	-1,00E+38	1,00E+25	-1,00E+38	99,5	100	-70,9	100
	O-PSO	72,449	72,4493	72,424	0,03606	0	50,71	-0,03	39,74
	DE	-8,524	12,054	-17,05	0,03125	59,596	65,44	59,87	0
	O-DE	72,453	72,453	72,452	0,0015	0	86,34	0	100

Source: By author, 2019.

Figures 6, 7, 8, and 9 show the PID controller response graphs for the step function and the P, I, and D parameters tuned by the algorithms PSO, O-PSO, DE and O-DE.

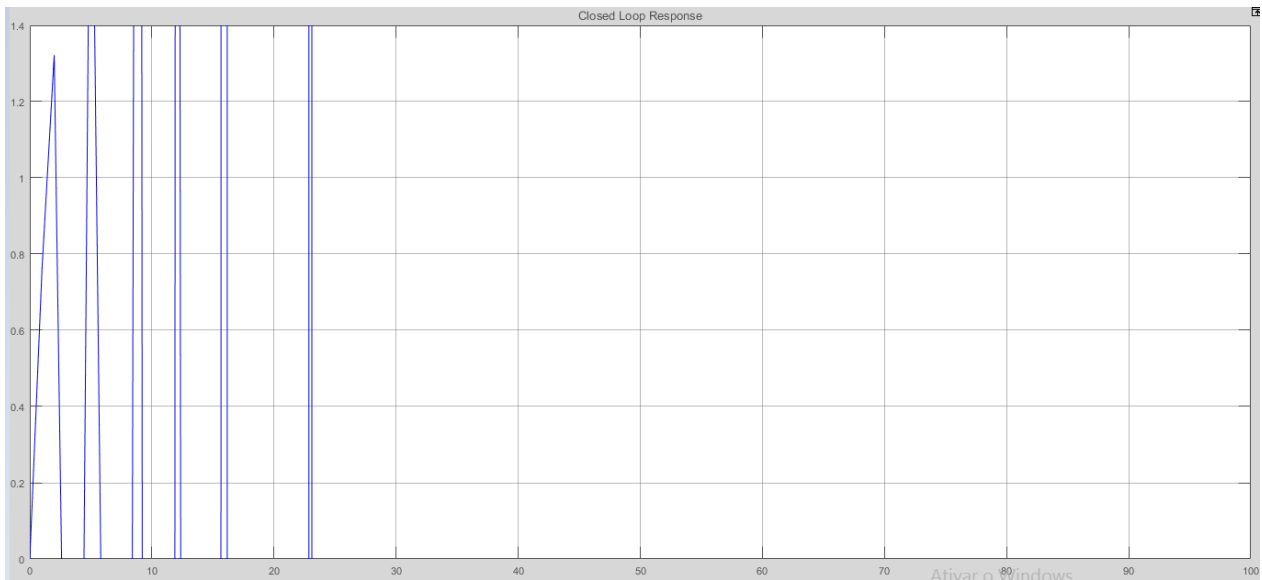


Figure 06 – PSO tuned controller response
 Source: By author, 2019.

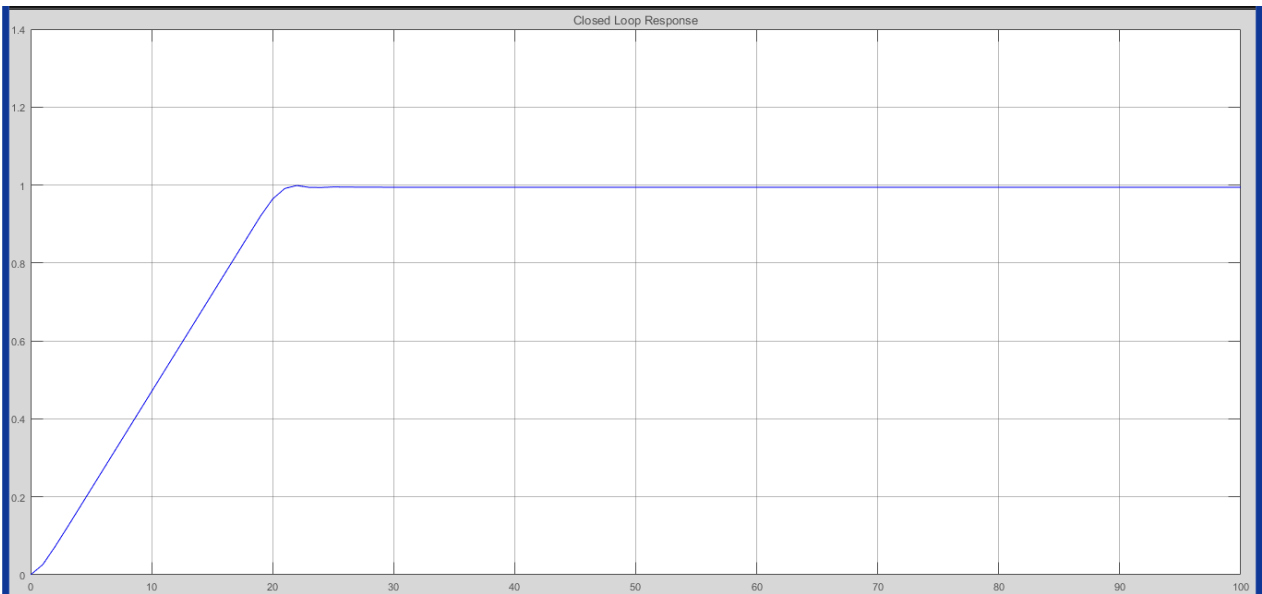


Figure 07 – Controller response tuned with O-PSO
 Source: By author, 2019.

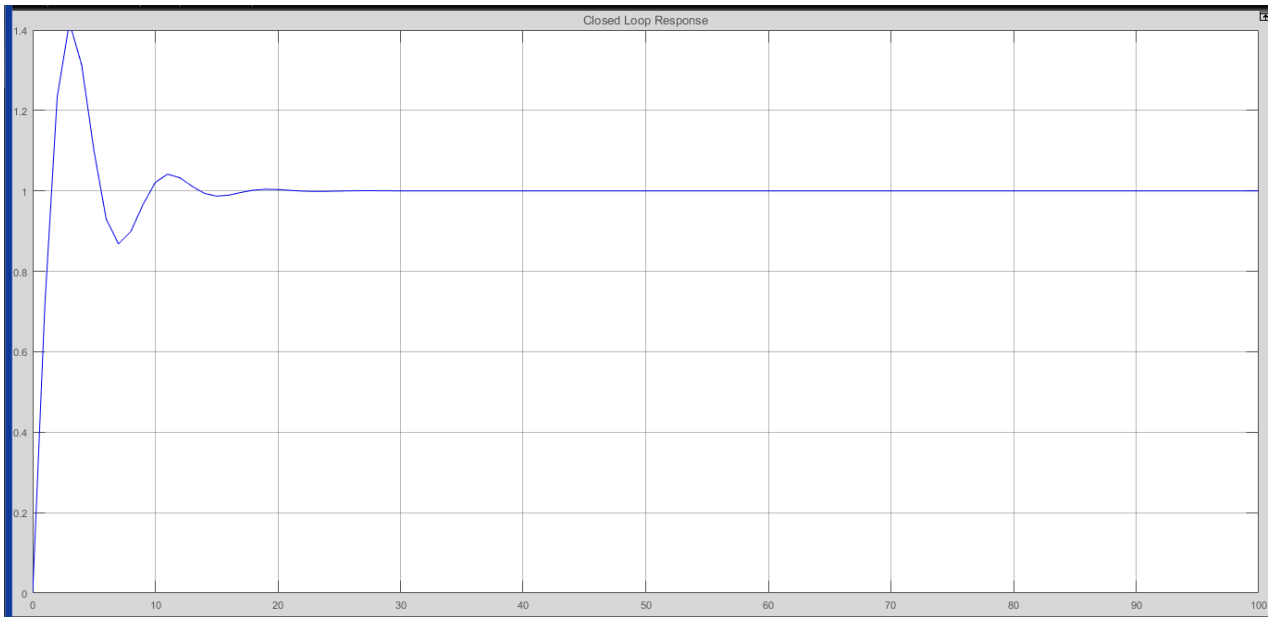


Figure 08 – Controller response tuned with DE
Source: By author, 2019.

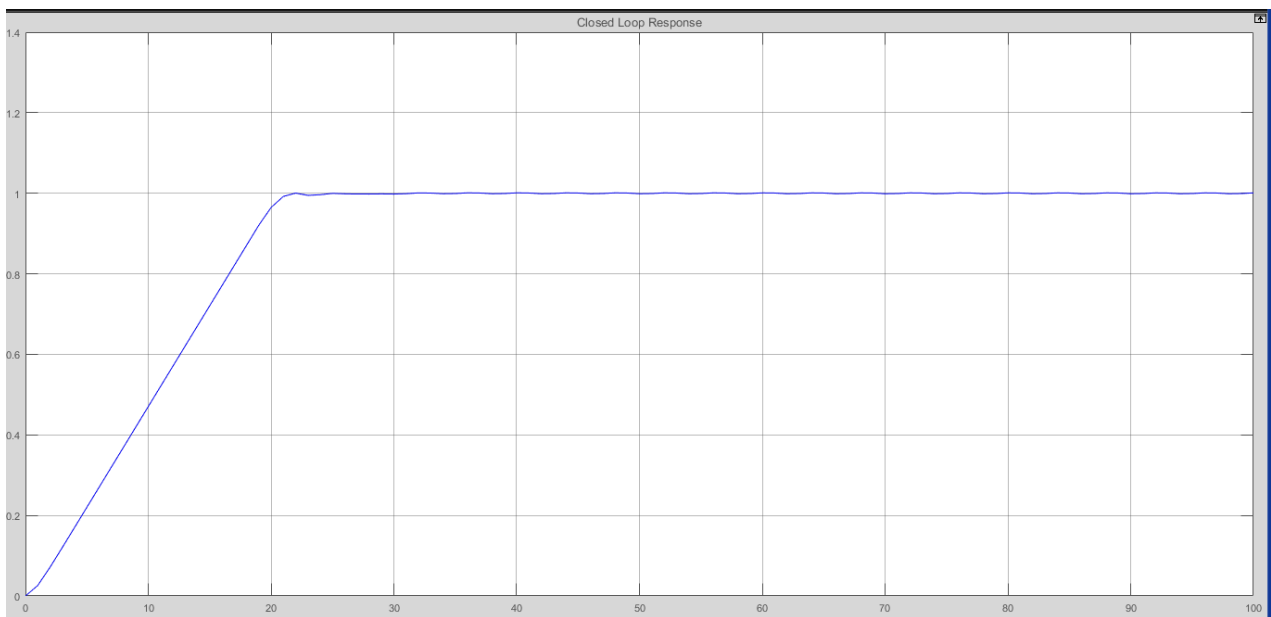


Figure 09 – Controller response tuned with O-DE
Source: By author, 2019.

3.1 Convergence Results

The experimental conditions for each algorithm are described in Table 01. The search spaces were limited according to Equation 8. The maximum allowable aptitude value (threshold) was set to 0.01 for the multimodal function.

Consistent with results described in Table 02; best overall position and the best aptitude obtained for each experiment, the mean value, median, standard deviation and the minimum aptitude value among all experiments were calculated, and the following considerations are presented for the experiments:

- Based on the average values in Table 02 and the graph in Figure 06, it can be stated that the PSO Algorithm does not provide satisfactory solutions for tuning the controller.
- Based on the average values of Table 02, standard deviation and the graphs of Figures 07 and 09, it can be stated that the O-PSO and O-DE algorithms provide satisfactory solutions for controller tuning. Increase and stabilization times are close to 20t, and the steady state error remains stable near value set point 1. The other observation is that the OBL learning variance favored the algorithms solution.

- Based on Table 02; median, standard deviation and the graph of Figure 08, it can be stated that the DE algorithm presents a satisfactory solution for the controller tuning. Increase times close to $3t$ and stabilization times less than $20t$ and steady state error remain stable near value set point 1. Since the integral component is displayed at relatively high values, a short increase time occurs and consequently overlaps, which for systems that require a short response time is satisfactory as long as the overlap is within acceptable parameters.
- The algorithm performance increases as the number of iterations increases, showing more adjusted P, I and D component values and consequent better step response.

4. RESULTS AND DISCUSSION OF TESTING OF COMPONENTS P, I AND D

In order to better observe the performance of the results found for the tests of the values of the variables P, I and D, Figures 10 and 11 graphically present the responses for path tracking and response time in frequency (Hz) and power control (kW). Data were extracted from the PI data acquisition tool - Plant Information; The software captures, processes, analyzes and stores any kind of data through information made available through graphic screens with data collected from the SDCD Digital Distributed Control System.

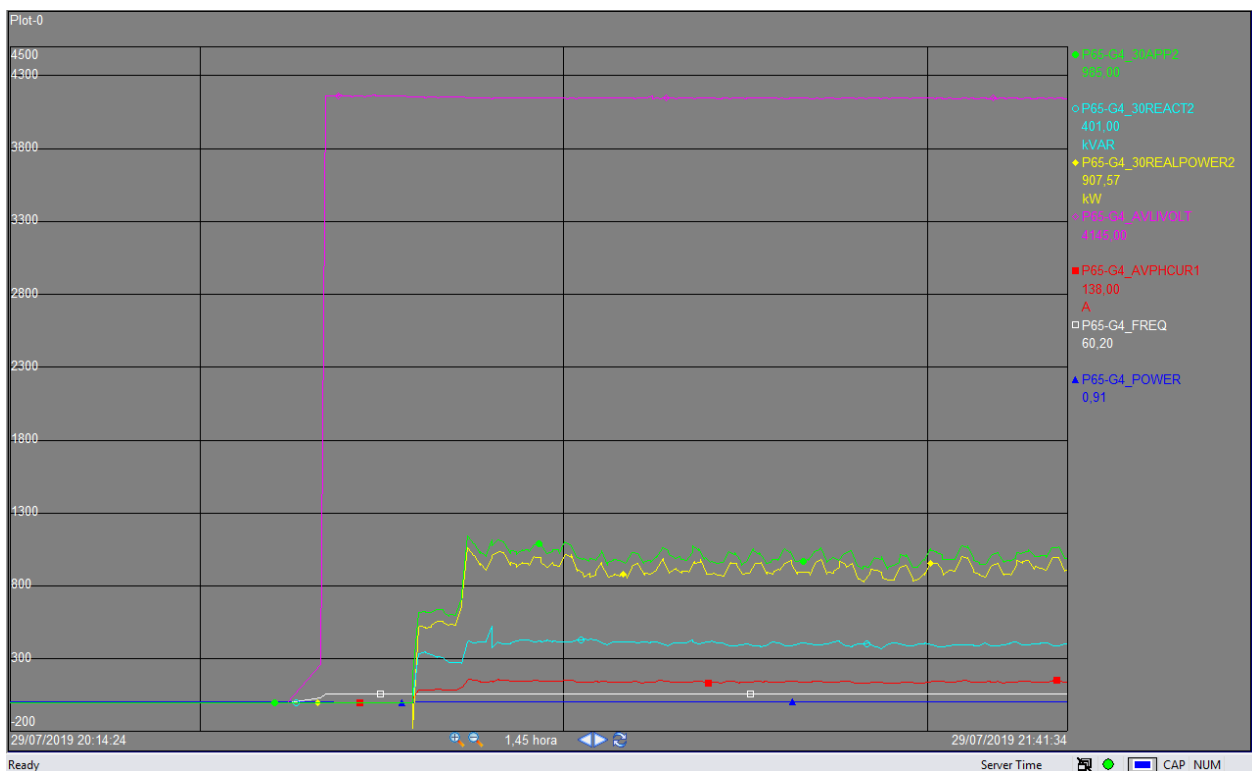


Figure 10 – DE-tuned controller response, time base 1.45h.
Source: By author, 2019.

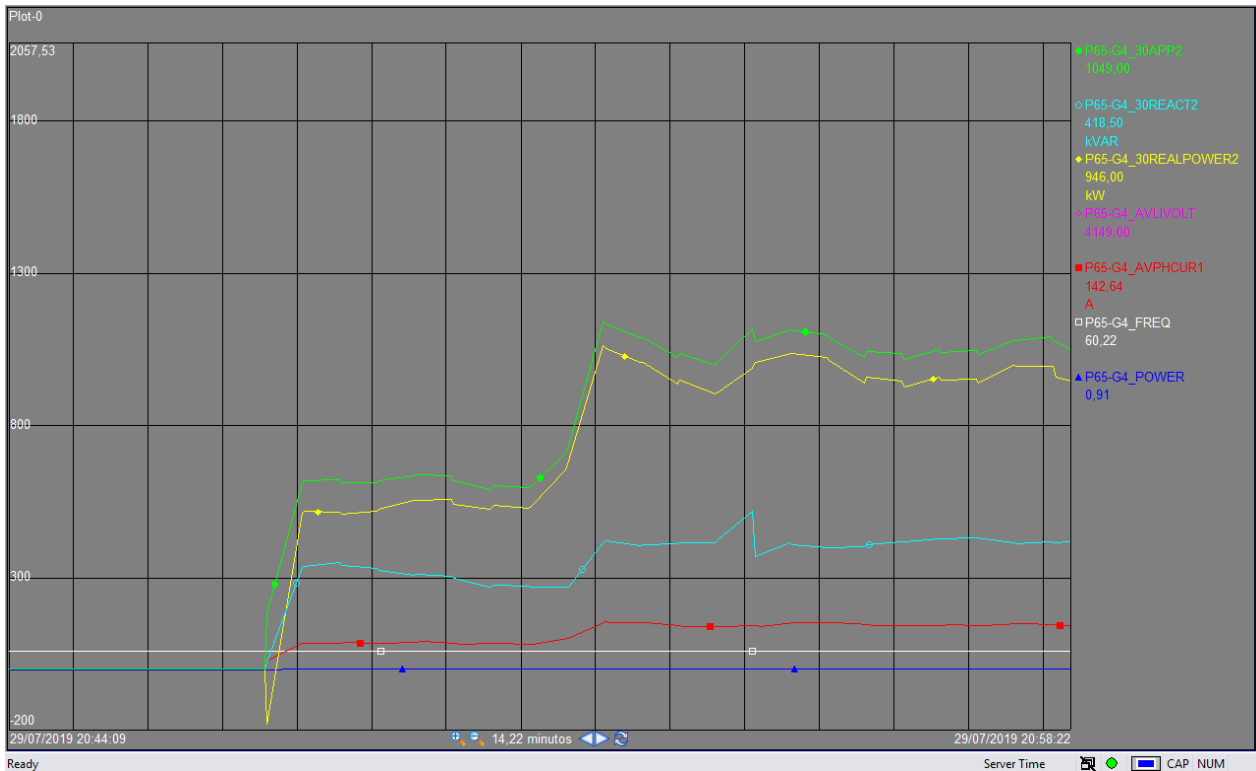


Figure 11 – DE-tuned controller response, timebase 14.22 minutes.
 Source: By author, 2019.

4.1 Convergence Results

For the tests initially a step function was applied, followed by a ramp function. The active power was oscillating near 946 kW, according to figures 10 and 11. The results shown refer to the best test response. The components were adjusted for the Proportional 65.44, Integral 59.87 and Derivative 0 tuning, thus a PI tuning obtained from experimental simulations.

Consistent with results shown in figures 10 and 11; path tracking for step function, path tracking for ramp function and response times, behavioral analysis of frequency (Hz), active power (kW), apparent power (kVA), reactive power (kVAR), current (A), voltage (VAC) and power factor, the following considerations are offered for the tests:

- Based on the average values of the graphs of Figures 10 and 11, it is possible to state that the tuning shown from the simulations with the DE algorithm presents satisfactory solutions for the control of the internal combustion motor-electric dynamometer system.
- Based on the path tracking at a step function of ~ 500 kW and the graphs in Figures 10 and 11, it can be stated that the controller has satisfactory system responses. The increase and stabilization times are close to 30s and steady state error remains stable near the 500 kW set point and there was no overlap. The other observation is that the power factor remained stable at 0.91, which indicates good power operation. The frequency remained stable near 60 Hz, indicating that the responses to the fuel injection advance signal to maintain engine dynamometer speed are satisfactory.
- Based on path tracking at a ~ 500 kW ramp function, reaching ~ 1000 kW and the graphs in Figures 10 and 11, it can be stated that the controller has satisfactory responses to the system. Increase times near 40s and stabilization times less than 20s and steady state error remain stable near the 1000 kW set point. Since the integral component is presented with relatively high values, there is a short increase time, and accordingly a small overlap, which for systems that require a short response time is satisfactory as long as the overlap is within acceptable parameters.
- Controller performance appears stable to fluctuations in the power system throughout the test while maintaining constant the speed of the internal combustion motor and stable frequency at 60 Hz.

5. CONCLUSIONS

The results achieved highlight an overview of the algorithm potential to solve multimodal optimization problems applied to tuning of PID controllers. In order to optimize performance it is possible to accomplish a process of adjusting the parameters of each algorithm. Additionally, increasing the number of iterations allows particles to have more

opportunities to converge to a solution. The solutions presented for the PID parameters in the controller tuning process associated with its motor-dynamometer cost function, using the O-PSO and evolution O-DE and DE algorithms are adequate. It was demonstrated that the DE tuning of the system controller parameters was the most efficient in the tests. The parameters defined for the PID components applied to the internal combustion motor (MCI)-electric dynamometer system controller for path tracking and response time tests are satisfactory for frequency (Hz) and power (kW) control. As future work, it is possible to expand the research and relate the reference curves of the MCI - Electric Dynamometer system with the transient tests standardized by national and international standards.

6. REFERENCES

- Diago, J.P. “*Otimização de controle de tráfego em grupo de elevadores com algoritmos bioinspirados*”. Dissertação de Mestrado em Sistemas Mecatrônicos, Publicação ENM.DM-088A/15, Departamento de Engenharia Mecânica, Universidade de Brasília, Brasília, DF, 2015, 105p.
- Eberhart, R.; Kennedy, J. "A new optimizer using particle swarm theory". *International Symposium Micro Machine and Human Science*. Nagoya, Japan: IEEE, 1995.
- Karaboga D.; Basturk, B. "A powerful and efficient algorithm for numerical function optimization: artificial bee colony (ABC) algorithm," *Journal of Global Optimization*, v. 39, 2007.
- Muñoz, D. “*Otimizacao por inteligencia de enxames usando arquiteturas paralelas para aplicacoes embarcadas*”. UnB- Universidade de Brasília, 2012.
- Quevedo, C. “*Notas de aula – Sistemas Sistema de Controle*”. UTFPR, 2012.
- Rahnamayan, S.; Tizhoosh, H.R.; Salama, M.M.A. “Opposition-based differential evolution for optimization of noisy problems”. In: *Proceedings of IEEE congress on evolution computation*, p. 1865–1872, 2006.
- Rahnamayan, S.; Tizhoosh, H.R.; Salama, M.M.A. “Opposition versus randomness in soft computing techniques”. *Elsevier J Appl Soft Comput*, v. 8, p. 906–918, 2008.
- Serapião, A.B. de Souza. “Fundamentos de otimização por inteligência de enxames: uma visão geral”. *Revista Controle & Automação*, v. 20, 2009.
- Storn, R.; Price, K. (1995). Differential evolution: a simple and efficient adaptive scheme for global optimization over continuous spaces, *Technical Report TR-95-012*, International Computer Science Institute, Berkeley.
- Shi, Y.; Eberhart, R. “A modied particle swarm optimizer”, *Proc. IEEE Congress on Computational Intelligence*, Anchorage, Alaska, USA, 1998. p. 69-73.

7. RESPONSIBILITY NOTICE

The authors is the only responsible for the printed material included in this paper.